Origin, fate and ecotoxicity of manganese from legacy metallurgical wastes

Quentin Petitjean, Flavien Choulet, Anne-Véronique Walter-Simonnet, Anne-Lise Mariet, Hervé Laurent, Patrick Rosenthal, Annette de Vaufleury, Frédéric Gimbert

Origin, fate and ecotoxicity of manganese from legacy metallurgical wastes.

Quentin Petitjean [a,1,2], Flavien Choulet [a], Anne-Véronique Walter-Simonnet [a], Anne-Lise Mariet [a], Hervé Laurent [b], Patrick Rosenthal [a], Annette de Vaufleury [a], Frédéric Gimbert [a*]

[a] *UMR CNRS 6249 Chrono-Environnement, Université Bourgogne Franche-Comté, Route de Gray, 25030 Besançon Cedex, France*

[b] *DRAC Bourgogne-Franche-Comté - site de Besançon, 7 rue Charles Nodier, 25043 Besançon Cedex, France.*

[1] *Laboratoire Ecologie Fonctionnelle et Environnement Ecolab UMR 5245, Université de Toulouse, CNRS, INPT, UPS, 118 route de Narbonne, 31062 Toulouse, France.*

[2] *Laboratoire Evolution et Diversité Biologique EDB UMR5174, Université de Toulouse, CNRS, ENFA, UPS, 118 route de Narbonne, 31062 Toulouse, France.*

** Corresponding author: Frédéric Gimbert, Tel.: +33 (0) 381 665 775; Fax: +33 (0) 381 666 568.*

E-mail address: frederic.gimbert@univ-fcomte.fr.

Abstract

Over the course of history, mining and metallurgical activities have influenced the socioeconomic development of human populations. However, these past and current activities can also lead to substantial environmental contamination by various metals. Here, we used an interdisciplinary approach (incorporating archaeology, mineralogy, environmental chemistry and ecotoxicology) to investigate the origin, fate and potential ecotoxicity of anomalous manganese (Mn) concentrations detected in the ancient mining district of Berthelange (medieval period, eastern France). Mineralogical investigations of slag samples showed that smelting temperature conditions in medieval bloomeries led to the production of slags mainly composed of Fe- and Mn-rich olivine, *i.e.*, fayalites. Further mineralogical analyses of bulk soil and clay fractions allowed us to identify the presence of serpentine. This evidence of olivine weathering can account for the release of Mn from slags into the soil. In addition, chemical analyses of total and available (exchangeable and reducible) Mn concentrations in soil samples clearly showed the contribution of slags deposited 1000 years ago to soil contamination. A complementary ecotoxicity bioassay performed on soils from a slag heap using the land snail *Cantareus aspersus* confirmed that a significant fraction of the Mn detected in soils remains available for partitioning with the soil solution and transfer to soil organisms. Although no growth inhibition of snails was observed after 28 days of exposure, the animals accumulated quite elevated Mn concentrations in their tissues. Our study emphasizes the environmental availability and bioavailability of Mn from ancient metallurgical wastes to soil-dwelling invertebrates, *i.e.*, snails, even one millennium after their deposition. Hence, as for more recent industrial sites, past mining ecosystems must be a cause of concern for the scientific community and public authorities.

Keywords (x6)

slags; weathering; metals; chemical extraction; bioavailability; snails

1. Introduction

Throughout human history, and especially since the Bronze Age, socioeconomic development has been strongly influenced by the exploitation of mineral resources, such as copper (Cu), iron (Fe), lead (Pb) or silver (Ag) (Nriagu, 1996; Tylecote, 1987). However, mineral-related activities also constitute the most ancient and significant source of waste production (Macklin et al., 1997; Pyatt et al., 2005). These types of wastes, originating from mining (ore dumps, ore-washing sediments) or metallurgical (smelter dusts, slags) operations, are currently considered archaeological clues. Until quite recently, slags were mostly considered chemically inert because of the strong association of metals with glass and mineral phases, limiting their lability (Wilson et al., 1994). However, a growing body of evidence shows that slags are affected by weathering and may be able to release metals into aquatic and terrestrial compartments (Ettler, 2002 and 2016; Gee et al., 1997; Lottermoser, 2002; Parsons et al., 2001; Piatak et al., 2004; Seignez et al., 2006).

In addition to the modification of the geochemical cycles of metals, this contamination may be responsible for the deterioration of water and soil quality and the impairment of biodiversity (Ettler et al., 2009; Lottermoser and Cairns, 2005). For instance, Monna et al. (2011) showed that wild brown trout living in past mining areas located in the Cevennes (France) were contaminated by Pb originating from historical activities (15^{th} and 20^{th} centuries). More recently, Mariet et al. (2016 and 2020) highlighted that metals originating from mining operations (Pb and Ag) during the end of the Middle Ages in the Vosges Mountains (France) remain bioavailable to soil invertebrates. However, the older the sites are, the scarcer the data are. In the Franche-Comté region (eastern France), Fe mining and metallurgical activities began in the Early Middle Ages (5^{th} century), with particular intensity in the district of Berthelange (Forlin and Laurent, 2014; Laurent, 2016). Until the 15^{th} century, a direct ore-reducing process was conducted within clay-made blast furnaces. In these

bloomeries, temperatures exceeded 1000°C, allowing, with the addition of charcoal, the reduction of Fe oxides (Fe_2O_3). At the end of the smelting process, a heterogeneous block of Fe (sponge) was kept for further purification, and metal-rich residues, *i.e.*, slags, were dumped on site as heaps. Currently, more than 1000 years later, the environmental effects of potential metal releases have, to our knowledge, not been evaluated.

Therefore, this study aims to assess the effect of very ancient slag deposits on soil quality. Because a single chemical analysis of total metal concentrations in soils may be insufficient for ecological risk assessment purposes (Peijnenburg, 2020), we combined physical, chemical and biological tools in a holistic approach. We operationally investigated the metal distribution in and transfer between various matrices (slags, soil and invertebrates) to reveal the origin, fate and effects of legacy contamination.

2. Materials and methods

2.1. Study area and sampling design

This study was performed in the Bourgogne Franche-Comté region of eastern France, where Fe mining and metallurgical exploitation were important activities during the Middle Ages (Jacob and Mangin, 1990). Over this period, Fe mining and metallurgical activities were particularly intense in the district of Berthelange (140 km², 20 km west from Besançon). The study area is composed of Jurassic limestones and marls (from Toarcian to Bajocian) partly covered by clay and sandy alluvial Pliocene deposits (Dreyfuss and Kuntz, 1967). Here, more than 120 direct Fe ore-reducing process sites were identified (Forlin and Laurent, 2014) because of the presence of slag repositories (from 10 to 20 m in diameter) (Figure 1A). In this study, eleven slag repositories, located in forested regions and well preserved, were investigated for the detection of potential anomalous metal concentrations in soils (Figure 1A,

Table 1). Among them, the Antorpe 9 heap (Figure 1B), containing slags produced during the 11th century (Forlin and Laurent, 2014), was selected for further investigations. More precisely, slags and soils were sampled using a transect method following four directions (NE, SE, SW and NW) from the centre of the slag heap (sampling point, SP, 4) according to Figure 1C. The reference site SP10 was located 100 m west of the heap. This remote station was selected to represent the pedogeological background of the area studied, *i.e.*, the same geological substrate and same vegetation cover, but without any smelting activities or slag deposit. At each sampling point, three soil cores (0-100 cm) were taken (after removing surface vegetation and humus) using a soil auger.

2.2. Soil analyses

2.2.1. Physico-chemical characterisation

The soil samples were primarily sieved (2 mm mesh; slag fragments were sorted for further analyses), dried at 40°C and homogenized. The soil pH was measured using a pH metre (WTW, pH/ION 3310) after extraction with demineralized water (1:5, v:v; ISO 10390, 2005), and the organic matter (OM) content was determined via the loss of ignition (LOI) method according to NF EN 15935 (AFNOR, 2013). Total metal concentrations were determined after hot mineralization in *aqua regia* (1:2.5 HNO_3: HCl, v:v) using a block digestion system (DigiPREP) and filtration (1 µm) by inductively coupled plasma atomic emission spectroscopy (ICP-AES) (Thermo Scientific, iCAP 6000 Series). The reliability of the analyses was assessed with certified reference material (calcareous loam soil: CRM n°141R from BCR). The recovery rate was on average 107±8% for all the metals analysed.

To identify potential decay products of slag minerals, mineralogical analyses of soil samples (bulk and clay fraction) from different depths (0-20 cm, 20-40 cm, 40-60 cm, 60-80

cm and 80-100 cm) were obtained using X-ray diffraction (XRD) characterization and a D8 Advance Bruker diffractometer equipped with a LinxEye detector (CuKα radiation at 1.54184 Å, 40 kV/40 mA) hosted at the Utinam Institute (University Bourgogne Franche-Comté, France). Powdered bulk rock samples were treated between 2θ values of 3° and 65° (divergent slit) with a step scan of 0.019° (2θ) and a scan rate of 1 s/step. The EVA software package was used for data processing and phase identification. The extraction of clay fractions required prior OM destruction by successive addition of 1 cm^3 hydrogen peroxide (33% H_2O_2, VWR Chemicals) to hydrated soil samples previously blended with water (1:5; w:v). To increase the reaction rate (Holtzapffel, 1985), this mixture was heated at 60°C on a digital hotplate (Stuart SD500).The samples were then subjected to repeated washing (n=4) using ultrapure water (UP) and centrifugation (10 min, 8,000 rpm). Afterward, clay suspensions were shaken in an end-over-end shaker for 10 min at 10 rpm. Finally, two clay fractions (<16 µm and <2 µm) were obtained by the sedimentation process according to Stoke's law, which links the settling rate to the particle size, and mounted on glass slides for XRD analyses. Before successive XRD analyses, the oriented preparations were sequentially air dried, glycolated and heated for 4 h at 490°C for identification of the interlayer of clays, *i.e.*, the (001) basal reflection positions after each treatment. The XRD patterns were obtained between 2° and 32° (2θ) with a step scan of 0.009° (2θ) and a scan rate of 1.5 s/step.

2.2.2. Environmental availability

The environmental availability was estimated using a chemical extraction method chosen to quantify the potential of metals for leaching or uptake by plants (Abedin et al., 2012). The extraction solution consisted of 1 $mol.L^{-1}$ ammonium acetate (NH_4OAc, purity >99%) added to a solution containing 2 $g.L^{-1}$ hydroxylamine hydrochloride salt (NH_2OH, HCl, purity >99%) and buffered at pH=7±0.05 using ammonium hydroxide (NH_4OH, purity >99%). Soil suspensions were obtained after shaking 37.5 mL of extraction solution and 1.5 g

149 of dried soil in an end-over-end shaker for 2 h at 10 rpm. Suspensions were then centrifuged
150 at 3000 rpm for 10 min and filtered through a 0.45 µm cellulose acetate disk filter to obtain
151 the extracts (AFNOR, 2002). To ensure complete extraction, the soil residues were subjected
152 to four successive extractions of 2 h each. Finally, metal concentrations were determined in
153 the total extract solutions by ICP-AES.

154

155 *2.3. Slag analyses*

156 2.3.1. Total metal concentrations

157 Total metal concentrations in slags (bulk) were determined according to the
158 international standard ISO 14869-1 (2001). Briefly, 0.250 g milled slag samples (n=3) were
159 digested in PTFE dishes on a hot plate (150°C) after the addition of 5 mL of hydrofluoric acid
160 (47% HF) and 1.5 mL of perchloric acid (65% $HClO_4$). The mixture was allowed to evaporate
161 to near complete dryness, and the residue was dissolved in diluted nitric acid (HNO_3) before
162 analysis by ICP-AES. The reliability of the analyses was assessed with certified reference
163 material (calcareous loam soil: CRM n°141R from BCR). The recovery rate averaged
164 104±6% for all the metals analysed.

165 2.3.2. Mineralogical characterisation

166 Slags were first ground, and the whole-rock powders were used for XRD analysis.
167 XRD patterns were obtained using the same method as for soil mineralogical characterisation
168 and allowed assessment of potential slag decay within soil through mineralogical analysis
169 (comparison of similar mineralogical phases within soil and slag samples).

170 Then, hand samples of slags were cut to prepare a 30 µm-thick polished thin section.
171 Optical investigations using scanning electron microscopy (SEM) in back-scattered electron
172 (BSE) mode were conducted at the Femto-ST Institute (University Bourgogne Franche-

Comté, France). Observations were complemented by energy-dispersive spectrometry (EDS) mapping obtained at the University of Lausanne (Switzerland) using a Tescan Mira LMU SEM equipped with a field emission gun (FEG). The composition of slag-forming minerals and glass were obtained by electron probe microanalysis (EPMA) at the University of Lausanne using a JEOL 8200 Superprobe equipped with five wavelength dispersion spectrometers (WDS). Carbon-coated polished thin sections were analysed with a 15 kV beam and a current of 15 nA. The resolution was ca. 1 µm. Oxides and silicates were used as standards. In addition, X-ray intensity mapping was carried out to reveal the specific textures caused by the chemical features of minerals.

2.4. Ecotoxicity test: snail growth inhibition and bioaccumulation

2.4.1. Animals

Land snails (*Cantareus aspersus*, Müller 1774, syn. *Helix aspersa*) were reared under controlled conditions according to Gomot-de Vaufleury (2000). For the bioassay, juvenile snails (n=105) were reared for 4 weeks and weighed 1.05±0.15 g prior to exposure.

2.4.2. Exposure modalities

Following the standard ISO 15952 (2018), the juvenile snails were exposed for 28 days to three surface soils (0-20 cm) originating from increasing distance to the centre of the smelting waste repository, *i.e.*, presenting a gradient in metal contamination (SP10, 8 and 4), and to a control treatment (C) in which snails were sustained over dampened absorbent paper. For each treatment, five transparent polystyrene containers of 3200 cm^3 (24 × 21 × 8 cm; ref. E1DBBAC001, Charles River IFFA-CREDO, 69 L'Arbresle) were used. Each container was filled with a 1.5 cm layer (200 g dry weight, DW) of soil or an absorbent paper layer, and five snails were introduced. The snails were fed ad libitum with uncontaminated Helixal® snail

197 food placed in a Petri dish left on the bottom of the container. The day/night cycle
198 photoperiod was 18/6 h, the temperature was 20±1°C, and the air relative humidity was
199 90±5%. Three times a week, the containers were cleaned, the faeces were removed, and the
200 food was renewed.

201 2.4.3. Measured endpoints

202 Each week, individual snail fresh mass (whole-body) and shell diameter were
203 monitored as biological endpoints for the assessment of sublethal effects.

204 At the end of the exposure, one snail was randomly sampled in each replicate
205 container for each exposure modality and subjected to a fasting period of 48 h to empty its gut
206 (the faeces were removed after 24 h to prevent their ingestion), then sacrificed by freezing at -
207 80°C. After thawing, the whole soft body was removed from the shell and separated into two
208 parts: the viscera (*i.e.*, the visceral complex containing the posterior gut, digestive gland,
209 kidney, mantle, and part of the reproductive tract) and the foot (containing the foot *sensu*
210 *stricto*, anterior gut, and remainder of the genital tract). The samples were then freeze-dried
211 and digested in HNO_3 (purity 99.9%) before analyses for metal content by ICP-AES. The
212 certified reference material was TORT-2 (lobster hepatopancreas from NRCC-CNRL,
213 Canada), and recovery rates ranged between 90% and 118% of the certified values for all the
214 metals.

215

216 *2.5. Statistics*

217 All data are presented as the mean ± standard deviation (sd). First, correlation analyses
218 were performed using the Spearman rank correlation test between the slag abundance
219 observed at each sampling point and physico-chemical parameters, such as the pH, OM
220 content and total and extractable metal concentrations.

Significant differences among soil parameters, metal concentrations, snail growth and metal bioaccumulation were then analysed by one-way analysis of variance (ANOVA) followed by Tukey's HSD post hoc test for pairwise comparisons. For the case in which the normality of distribution and homogeneity of variances were not verified (using the Shapiro–Wilk and Bartlett tests, respectively), the Kruskal-Wallis test followed by the Kruskalmc post hoc test (pgirmess package) were used. For all statistical analyses, a *p*-value of 5% was used as a significance threshold.

All statistical analyses were performed with the free statistical software R (ver 3.4.0) (R Core Team, 2020).

3. Results

3.1. Soil contamination in the Berthelange district

Metal concentrations in soils formed above the slag heaps and in reference soils, *i.e.*, soils that had never been subject to metallurgical activities, are presented in Table 1. In the reference sites, metal concentrations are relatively low in comparison with values measured on slag repositories. Indeed, among the metals that have been analysed, some exceed the maximum permissible concentrations in soils. For instance, low anomalous concentrations are observed for arsenic (As) and zinc (Zn) in Petit-Mercey 25, Antorpe 9 or Ferrières 8. The most marked contamination concerns major elements, such as Fe and Mn, with total concentrations in soils of the latter element reaching more than 8500 $\mu g.g^{-1}$ at the Antorpe 9 site. Therefore, further results and discussion will focus particularly on this site and this element.

3.2. Characterisation of slags

245 At the macroscopic scale, slags from the Antorpe 9 heap are generally homogeneous
246 in shape, density and porosity. The morphology directly reflects the smelting technology in
247 bloomeries. Slags are generally dark-coloured, ranging from blueish to brownish. Flow
248 texture is frequently observed and is characteristic of slags formed in a molten state. Vesicles,
249 ranging from micrometres to centimetres, are commonly met.

250 Metal concentrations in slags of Antorpe 9 (Table 1) reach an average of
251 approximately 15% Fe and 1.7%, 1.5% and 0.35% Mn, Ca and Mg, respectively. Other
252 quantified trace metal elements present lower concentrations ranging between 0.0003% (for
253 cadmium, Cd) and 0.008% (for Cu). At the mineralogical scale, XRD patterns allowed us to
254 identify fayalite, an olivine group mineral, as the main component of slags (Figure 2A).
255 Petrographic investigations on polished thin sections showed that the phases present in
256 Antorpe 9 slags include olivine, glass, spinel, leucite, wustite and metallic Fe (Figure 3).
257 Olivine group minerals commonly display a spinifex texture and elongated skeletal laths; the
258 WDS analyses revealed a fayalite (Fe_2SiO_4) composition. The glass phase is generally
259 interstitial and contains subhedral spinel crystals (Figure 3B). Locally, wustite occurs as bleb
260 aggregates and is partially replaced by secondary Fe phases. Similarly, metallic Fe fragments
261 are corroded and transformed into oxides and hydroxides (Figure 3D). As shown in Table 2,
262 Mn is heterogeneously distributed between minerals and glass. Fayalite, which may contain
263 up to 5% MnO, is the primary carrier of Mn, while glass and spinel display MnO contents of
264 less than 1.8% (Table 2; Figure 3C). Manganese is almost absent in metallic Fe and secondary
265 Fe phases (Figure 3F).

266

267 *3.3. Influence of the slag heap on soil characteristics*

268 The edges of the heap were delimited using the relative abundance of slags in the
269 surface layer (0-20 cm) of soils collected at each sampling point (Figure 4). Regardless of the

transect direction considered, the slag abundance decreases with the distance from the centre of the heap, dropping from approximately 70% at SP4 to less than 5% at the heap foot (SP3, 5, 7 and 8).

Significant positive correlations were identified between the slag abundance and some physicochemical parameters of soils (Figure 4), such as the OM content (Rho=0.94, $p<0.001$) and pH (Rho=0.54, $p<0.001$). Indeed, from the edge of the slag heap to its centre, the OM content and pH values increase from 8 to 19% and 4.8 to 5.4, respectively.

Variations in the clay composition of soils are also observed by means of XRD analyses of soils (Figure 2B) and clay extract (Figures 2C to G). Mineralogical analyses of clay extract from soil samples allowed us to identify different clay minerals that are present in various proportions depending on the samples: illite, chlorite, kaolinite, serpentine (antigorite/chrysotile), and mixed-layer clay minerals. Kaolinite and serpentine exhibit very similar diffraction patterns, but the absence of tetrahedral substitution in antigorite and chrysotile induces rolling up of the layers (Holtzapffel, 1985; Moore and Reynolds, 1997). This characteristic allowed us to distinguish samples without serpentine (Figure 2E) from samples containing serpentine (Figures 2F and G).

The total Mn concentrations in the soils range from 1150 $\mu g.g^{-1}$ at the reference site (SP10) to approximately 3500 $\mu g.g^{-1}$ at the heap foot (SP3, 7 and 8) and up to more than 8000 $\mu g.g^{-1}$ at the centre of the heap (SP4) (Figure 4). Manganese extractable concentrations display a similar pattern to total Mn with increasing values from SP10 (880 $\mu g.g^{-1}$) to SP4 (2800 $\mu g.g^{-1}$), representing extraction yields of 77% and 35%, respectively. Surprisingly, at SP9, the total and extractable concentrations were particularly low, *i.e.*, 400 and 170 $\mu g.g^{-1}$, respectively.

294 *3.4. Ecotoxicological bioassay*

295 No snail mortality was recorded over the 28-day exposure periods. Concerning
296 sublethal effects, the growth of snails exposed to the four modalities did not show any
297 significant difference either in terms of body mass (Figure 5A) or shell diameter (data not
298 shown). Indeed, the final mass of snails reached 6.9 ± 1.2 g for the control modality and 7.3 ±
299 1.4 g, 7.2 ± 1.6 g and 7.2 ± 1.1 g for snails exposed to soils located at 100 m, 5 m and the
300 centre of the heap, respectively. Similarly, the final shell diameter increased 28.12 ± 3.0 mm
301 for the control and 28.85 ± 2.38 mm, 28.92 ± 2.52 mm, and 29.29 ± 1.97 mm for snails
302 exposed to the three previously cited soils.

303 Growth measurements were completed with Mn bioaccumulation data in snail foot
304 and viscera after 28 days of exposure (Figure 5B). As snails grew over the 28-day duration of
305 the exposure, we used body burdens rather than tissue concentrations because the latter can be
306 affected by rapid changes in the mass of the organism (Gimbert et al., 2006; Gimbert and de
307 Vaufleury, 2009). Snails significantly accumulate Mn in their viscera following a dose-
308 response pattern according to the Mn concentrations in soils. Viscera internal burdens reached
309 25.2 ± 8.3 µg in the control snails (*i.e.*, snail food exposure only) and 93.4 ± 1.1 µg, 93.5 ±
310 29.6 µg and 154.0 ± 34.4 µg in snails exposed to soils from SP10, SP8 and SP4, respectively.
311 Accumulation in the foot is low, and body burdens do not vary regardless of the exposure
312 modality (Figure 5B).

313

314 **4. Discussion**

315 *4.1. Source of Mn contamination in soils*

316 Manganese concentrations measured in reference soils from the study area average
317 approximately 800 $\mu g.g^{-1}$ and are in accordance with the Mn pedogeochemical background of

soils (Pinsino et al., 2012; Grygo-Szymanko et al., 2016). Varying from 480 to 1150 $\mu g.g^{-1}$, these background concentrations nevertheless show a spatial heterogeneity that has to be related to the lithological nature of the soils (including within the same geological formation) and to the local soil features (both abiotic and biotic). However, this natural variability is not of the same order of magnitude as what is observed in soils formed on ancient slag repositories. Indeed, Mn concentrations range from 1200 to more than 8000 $\mu g.g^{-1}$, testifying to the influence of smelting wastes on soil contamination. These values exceed the maximum permissible concentrations in soils; therefore, it is necessary to better understand the origin and fate of this element in past mining ecosystems.

In slags, three main mineralogical phases are identified: metallic Fe residues, glass and fayalites belonging to the olivine group. The presence of metallic Fe inclusions in slags attests to the generally moderate extraction yields of Fe during the Early Middle Ages. Glass is ubiquitous in slags from Antorpe 9 and is primarily composed of Si, Ca and Al oxides, as reported in the literature (Piatak et al., 2015). The presence of fayalite and its dendritic shape are related to the temperature in the bloomeries (reaching more than 1000°C) and the slow air-cooling conditions of molten slags at the end of the smelting process (Piatak et al., 2004; Tossavainen et al., 2007). The manganese concentration is 1.7% in slag bulk samples and is primarily located in fayalites, where it reaches 4.5 wt.% MnO. In their review, Piatak et al. (2015) provided average concentrations of Mn in steel and pre-1900 and modern Fe slags between 1 and 4 wt.% MnO.

The weathering of the slag primary phases after abiotic (air or water) or biotic (microorganisms) interactions leads to the production of secondary products that can be used as indicators of the reactivity and alteration of slags (Piatak et al., 2015). In Antorpe 9 soils, three clues of slag alteration have been identified. First, the alkalization of soil (+ 0.6 pH unit between the reference soil and the centre of the heap) may originate from the hydrolysis of CaO and other Ca-Mg oxide and silicate phases of slags and the subsequent release of Ca^{2+} and hydroxyl (OH^-) ions (Riley and Mayes, 2015; Roadcap et al., 2006). This well-known phenomenon led to the use of slags as a liming agent for soil quality restoration (Lopez et al., 1995; Pinto et al., 1995). Second, we identified serpentine minerals ((Mg, Fe, Ni, Mn, Al, Zn) $[Si_2O_5]$ $(OH)_4$) in soils from Antorpe 9 slag heap. Serpentine is a subgroup of minerals belonging to the kaolinite-serpentine group and usually contains divalent cations in octahedrally coordinated sites. This type of mineral is frequently formed after weathering of olivine in rocks. This serpentinization process is also known for magnesiferous olivines in geological environments (basaltic rock alteration; Muntener, 2010), as well as for zinciferous silicates in surface conditions (Choulet et al., 2016); to our knowledge, the process is rarely demonstrated for ferriferous and manganiferous olivines. Finally, along with alkalization and serpentinization, Mn can be considered a release product of slag weathering leading to soil contamination.

From an environmental point of view, this soil contamination raises the question of mobility and potential transfers to abiotic and biotic compartments of the current ecosystem. Chemical extraction using ammonium acetate and hydroxylamine hydrochloride allowed us to estimate the environmental availability of Mn in soils from Antorpe 9. This extractant can extract the exchangeable metal fraction (including water-soluble Mn held on the surface of negatively charged exchange complexes and Mn coprecipitated with the carbonate fraction) and the easily reducible fraction (including oxides) (McAlister and Smith, 1999). This result

363 explains the elevated Mn extraction yields in the reference soil (77%, *i.e.*, 880 µg.g^{-1}). In slag-
364 impacted soils, Mn availability is higher and increases from the edge (approximately 1600
365 µg.g^{-1}) to the centre of the heap (2800 µg.g^{-1}). In contrast, the extraction yields decreased,
366 ranging from 66 to 35%. This result may be related to the fractionation of Mn, which relies on
367 (i) the soil characteristics affected by the slag deposit (*i.e.*, alkaline soil pH, high OM and clay
368 content) (Walna et al., 2010) and (ii) the sequestration of a substantial portion of the total Mn
369 concentrations in a soil fraction refractory to the extraction (*i.e.*, the mineral matrix) (Maskall
370 et al., 1995). We have recently confirmed these findings with an in-depth study of the Mn
371 partitioning in soils from Roman and medieval slag heaps (Amnai et al., 2021). We have
372 indeed demonstrated that Mn was mainly found in the reducible (oxides) and residual (slag
373 micro-fragments) fractions of soils. The anomalously low total and extractable concentrations
374 at SP9 may hence be explained by its localization in the vicinity of a small pond, which
375 modifies the hydromorphic conditions of soil (*i.e.*, decreases the redox potential) and
376 subsequently promotes the leaching of Mn (Walna et al., 2010).

377

378 *4.2. Manganese bioavailability, transfer and toxicity*

379 The terrestrial snail *Cantareus aspersus* is well recognized as a biological indicator (de
380 Vaufleury, 2015), integrating three contamination routes: respiratory (from atmospheric
381 sources), digestive (from plant and soil sources) and dermal (diffusion of metals through the
382 foot epithelium). In addition to the chemical assessment of metal environmental availability,
383 the analysis of metal bioaccumulation in snail tissues constitutes a way to estimate the
384 fraction of the total concentration in soil that is truly transferable in biota, *i.e.*, the metal
385 bioavailability (ISO 17402, 2008). The snail foot is primarily composed of muscles and does
386 not appear, as for other trace elements, to be an important sink for Mn (de Vaufleury et al.,
387 2006). In viscera, the digestive gland (or hepatopancreas) is the main storage organ of Mn,

especially in intracellular granules occurring in large numbers in basophil cells (Mason and Simkiss, 1982). The Mn burdens accumulated in snail viscera are in accordance with extractable concentrations and confirm that a substantial portion of the Mn released by slags is effectively bioavailable to soil organisms and particularly snails. Despite the high total and available Mn exposure concentrations in soils, we did not observe deleterious effects regarding snail survival or growth, as already noticed with artificially contaminated soils (up to 750 µg $Mn.g^{-1}$ soil; Bordean et al., 2014). These results are not obvious with respect to ecotoxicity data available in the literature. Indeed, Kuperman et al. (2004) determined laboratory LC_{50} values (concentrations in the soil causing 50% mortality) of 389 $\mu g.g^{-1}$, 1970 $\mu g.g^{-1}$ and 2575 $\mu g.g^{-1}$ for *Enchytraeus crypticus, Eisenia fetida and Folsomia candida*, respectively. The absence of significant detrimental effects on snails may be related to (i) a misestimation of toxicity metrics estimated using spiked artificial soils (Lock and Janssen, 2001); (ii) the presence in field soils of growth-promoting factors for snails, such as humic substances and oligo-elements (Gomot et al., 1989); and (iii) the ability of *C. aspersus* snails to accumulate and detoxify Mn in their tissues using detoxification processes, such as metal-rich granules (Mason and Simkiss, 1982; Simkiss and Taylor, 1994). However, other sensitive biomarkers at the cellular and subcellular levels (*e.g.*, cytotoxicity; Bradley and Runham, 1996) deserve to be investigated. At the ecosystem scale, snails, as possible prey for numerous invertebrates and vertebrates, may contribute to the diffusion of metals in trophic chains (Moreno-Jiménez et al., 2011).

5. Conclusion

Although slag heaps may be regarded as punctual sources of metal release, their very large number, considerable cumulative volume and spatial coverage make them a significant

source of risk (Amnai et al., 2021). The combination of mineralogical, chemical and ecotoxicological approaches allows us to show here that, in addition to the modification of various soil physico-chemical characteristics, such as the pH and OM content, slag weathering over centuries led to the release of metallic contaminants in the surrounding environment. Among them, Mn ranks, based on a combination of its frequency, toxicity, and potential for human exposure, 140th (out of 275) in the substance priority list of the Agency for Toxic Substances and Disease Registry (ATSDR, 2019). We have emphasised not only the environmental availability of this metallic palaeo-pollution but also its bioavailability to soil-dwelling invertebrates, such as snails. Hence, such legacy contaminated sites need to be more clearly identified and included in environmental risk assessment procedures.

Acknowledgements

The authors warmly thank N. Crini, C. Amiot, M. Perrey and D. Convert from the PEA²t platform (Chrono-environment, University of Bourgogne Franche-Comté, France), which manages and maintains most of the analytical equipment used in this study. We are also grateful to P. Vonlanthen (University of Lausanne) for his technical assistance using EPMA. B. Pauget, C. Lobjoie, G. Link and R. Nazir are also acknowledged for fruitful discussions about the results. Financial support was provided by the Région Bourgogne Franche-Comté (programs SIDEROS and ALTERICS, coord.: F. Gimbert and F. Choulet, respectively).

References

435 Abedin, J., Beckett, P., Spiers, G., 2012. An evaluation of extractants for assessment of metal
436 phytoavailability to guide reclamation practices in acidic soilscapes in northern regions.
437 Can. J. Soil Sci. 92, 253-268. doi:10.4141/CJSS2010-061

438 AFNOR, 2013. Boues, bio-déchets traités, sols et déchets - Détermination de la perte au feu -
439 NF EN 15935. Paris, France : Association Française de Normalisation.

440 AFNOR, 2002. Qualité des sols - Détermination des cations Ca++, Mg++, K+, Na+
441 extractibles par l'acétate d'ammonium - Méthode par agitation - NF X31-108. Paris,
442 France: Association Française de Normalisation.

443 Bordean, D.M., Nica, D.V., Harmanescu, M., Banatean-Dunea, I., Gergen, I.I., 2014. Soil
444 Manganese Enrichment from Industrial Inputs: A Gastropod Perspective. PLoS ONE 9,
445 e85384. doi:10.1371/journal.pone.0085384

446 Bradley, M.D., Runham, N.W., 1996. Heavy metal toxicity in the snail Helix aspersa maxima
447 reared on commercial farms: cellular pathology. In: Henderson IF, editor. Slug and snail
448 pests in agriculture: Proceedings of a Symposium Held at the University of Kent: 24–26
449 September 1996. Canterbury: British Crop Protection Enterprises, 353–358.

450 Choulet, F., Buatier, M., Barbanson, L., Guégan, R., Ennaciri, A., 2016. Zinc-rich clays in
451 supergene non-sulfide zinc deposits. Miner. Deposita 51, 467–490. doi:10.1007/s00126-
452 015-0618-8

453 Crommentuijn, T., Sijm, D., de Bruijn, J., van den Hoop, M., van Leeuwen, K., van de
454 Plassche, E., 2000. Maximum permissible and negligible concentrations for metals and
455 metalloids in the Netherlands, taking into account background concentrations. J. Environ.
456 Manage. 60, 121–143. doi:10.1006/jema.2000.0354

457 de Vaufleury, A., 2015. Landsnail for Ecotoxicological Assessment of Chemicals and Soil
458 Contamination – Ecotoxicological Assessment of Chemicals and Contaminated Soils
459 Using the Terrestrial Snail, Helix aspersa, at Various Stage of Its Life Cycle: A Review, in:
460 Environmental Indicators. Springer, Dordrecht, 365–391.

461 de Vaufleury, A., Coeurdassier, M., Pandard, P., Scheifler, R., Lovy, C., Crini, N., Badot,
462 P.M., 2006. How terrestrial snails can be used in risk assessment of soils. Environ.
463 Toxicol. Chem. 25, 797–806. doi:10.1897/04-560R.1

464 Dreyfuss, M. and Kuntz, G., 1967. Carte au 1/50 000 et notice géologiques de Besançon.
465 Editions du BRGM.

466 Ettler, V., 2002. Leaching of polished sections: an integrated approach for studying the
467 liberation of heavy metals from lead-zinc metallurgical slags. Bull. Soc. Geol. Fr. 173,
468 161–169. doi:10.2113/173.2.161

469 Ettler, V., 2016. Soil contamination near non-ferrous metal smelters: A review. Applied
470 Geochemistry 64, 56-74. doi: 10.1016/j.apgeochem.2015.09.020

471 Ettler, V., Johan, Z., Kříbek, B., Šebek, O., Mihaljevič, M., 2009. Mineralogy and
472 environmental stability of slags from the Tsumeb smelter, Namibia. Appl. Geochem. 24,
473 1–15. doi:10.1016/j.apgeochem.2008.10.003

474 Forlin, P., Laurent, H., 2014. Exploiting local resources in a new economic frame: iron ores
475 and bloomeries in Franche-Comté (F) during the early middle ages. In: Research and
476 preservation of ancient mining areas, 9th International Symposium on archaeological
477 Mining History (Trento), Yearbook of the Institute Europa Subterranea, edited by
478 Silvertant MA, Trento/Valkenburg de Geul, 2014, 196–217.

Gee, C., Ramsey, M.H., Maskall, J., Thornton, I., 1997. Mineralogy and weathering processes in historical smelting slags and their effect on the mobilisation of lead. J. Geochem. Explor. 58, 249–257. doi : 10.1016/S0375-6742(96)00062-3

Gimbert, F., de Vaufleury, A., 2009. Bioindication et unités (concentrations vs quantités). Étude et Gestion des Sols 16, 243–252.

Gimbert, F., de Vaufleury, A., Douay, F., Scheifler, R., Coeurdassier, M., Badot, P.M., 2006. Modelling chronic exposure to contaminated soil: A toxicokinetic approach with the terrestrial snail Helix aspersa. Environ. Int. 32, 866–875. doi:10.1016/j.envint.2006.05.006

Gomot, A., Gomot, L., Boukraa, S., Bruckert, S., 1989. Influence of soil on the growth of the land snail Helix aspersa. An experimental study of the absorption route for the stimulating factors. J. Molluscan Stud. 55, 1–7. doi: 10.1093/mollus/55.1.1-a

Gomot-de Vaufleury, A., 2000. Standardized Growth Toxicity Testing (Cu, Zn, Pb, and Pentachlorophenol) with *Helix aspersa*. Ecotoxicol. Environ. Saf. 46, 41–50. doi:10.1006/eesa.1999.1872

Grygo-Szymanko, E., Tobiasz, A., Walas, S., 2016. Speciation analysis and fractionation of manganese: A review. Trends in Analytical Chemistry 80, 112-124. doi: 10.1016/j.trac.2015.09.010

Holtzapffel, T., 1985. Les minéraux argileux: préparation, analyse diffractométrique et détermination. Société géologique du Nord 12, pp.136.

ISO 10390, 2005. Soil quality - Determination of pH, Geneva, Switzerland: International Organization for Standardization.

ISO 14869-1, 2001. Soil quality - Dissolution for the determination of total element content -- Part 1: Dissolution with hydrofluoric and perchloric acids, International Organization for Standardization, Geneva, Switzerland.

ISO 15952, 2018. Soil quality - Effects of pollutants on juvenile land snails (Helicidae) -- determination of the effects on growth by soil contamination, International Organization for Standardization, Geneva, Switzerland.

ISO 17402, 2008. Soil quality - Guidance for the selection and application of methods for the assessment of bioavailability of contaminants in soil and soil materials. (International Organization of Standardization).

Jacob, J.P., Mangin, M., 1990. De la mine à la forge en Franche-Comté: des origines au XIXe siècle. Editions Belles Lettres, Collection Annales littéraires de l'Université de Besançon, France. p. 318.

Kuperman, R., Checkai, R., Simini, M., Phillips, C., 2004. Manganese toxicity in soil for Eisenia fetida, Enchytraeus crypticus (Oligochaeta), and Folsomia candida (Collembola). Ecotoxicol. Environ. Saf. 57, 48–53. doi:10.1016/j.ecoenv.2003.08.010

Laurent H., 2016. La métallurgie : réduction et forge en Franche-Comté à la fin de l'Antiquité et pendant la période mérovingienne. Chap. 4-1. In: Billoin D., L'établissement de Pratz « Le Curtillet ». Un domaine mérovingien dans les hautes terres jurassiennes (fin VIe-VIIe siècles). Editions INRAP-CNRS, Collection Recherches Archéologiques, pp. 310.

Lock, K., Janssen, C.R., 2001. Ecotoxicity of Zinc in Spiked Artificial Soils versus Contaminated Field Soils. Environ. Sci. Technol. 35, 4295–4300. doi: 10.1021/es0100219

521 Lopez, F.A., Balcazar, N., Formoso, A., Pinto, M., Rodriguez, M., 1995. The recycling of
522 Linz-Donawitz (LD) converter slag by use as a liming agent on pasture land. Waste
523 Manag. Res. 13, 555–568. doi: 10.1006/wmre.1995.0052

524 Lottermoser, B.G., 2002. Mobilization of heavy metals from historical smelting slag dumps,
525 north Queensland, Australia. Mineral. Mag. 66, 475–490. doi:10.1180/0026461026640043

526 Lottermoser, B.G., Cairns, 2005. Evaporative mineral precipitates from a historical smelting
527 slag dump, Río Tinto, Spain. Neues Jahrb. Für Mineral. - Abh. 181, 183–190.
528 doi:10.1127/0077-7757/2005/0016

529 Macklin, M., Hudson-Edwards, K., Dawson, E.J., 1997. The significance of pollution from
530 historic metal mining in the Pennine ore fields on river contaminant fluxes to the North
531 Sea. Sci. Total Environ. 194-195, 391–397. doi:10.1016/S0048-9697(96)05378-8

532 Mariet, A.L., de Vaufleury, A., Bégeot, C., Walter-Simonnet, A.V., Gimbert, F., 2016.
533 Palaeo-pollution from mining activities in the Vosges Mountains: 1000 years and still
534 bioavailable. Environ. Pollut. 214, 575–584. doi:10.1016/j.envpol.2016.04.073

535 Mariet, A.L., Gauthier-Manuel, H., Lagiewski, T., Bégeot, C., Walter-Simonnet, A.V.,
536 Gimbert, F., 2020. Impact assessment of legacy wastes from ancient mining activities on
537 current earthworm community. J. Haz. Mat. 393, 122369. doi:
538 10.1016/j.jhazmat.2020.122369

539 Maskall, J., Whitehead, K., Thornton, I., 1995. Heavy metal migration in soils and rocks at
540 historical smelting sites. Environ. Geochem. Health 17, 127–138. doi:
541 10.1007/BF00126081

542 Mason, A.Z., Simkiss, K., 1982. Sites of mineral deposition in metal-accumulating cells. Exp.
543 Cell Res. 139, 383–391. doi:10.1016/0014-4827(82)90263-4

McAlister, J., Smith, B., 1999. Selectivity of Ammonium Acetate, Hydroxylamine Hydrochloride, and Oxalate/Ascorbic Acid Solutions for the Speciation of Fe, Mn, Zn, Cu, Ni, and Al in Early Tertiary Paleosols. Microchem. J. 63, 415–426. doi:10.1006/mchj.1999.1798

Monna, F., Camizuli, E., Revelli, P., Biville, C., Thomas, C., Losno, R., Scheifler, R., Bruguier, O., Baron, S., Chateau, C., Ploquin, A., Alibert, P., 2011. Wild Brown Trout Affected by Historical Mining in the Cévennes National Park, France. Environ. Sci. Technol. 45, 6823–6830. doi:10.1021/es200755n

Moore, DM. and Reynolds, RC., 1997. X-Ray Diffraction and the Identification and Analysis of Clay Minerals. Oxford University Press, Oxford, 378p.

Moreno-Jiménez, E., García-Gómez, C., Oropesa, A.L., Esteban, E., Haro, A., Carpena-Ruiz, R., Tarazona, J.V., Peñalosa, J.M., Fernández, M.D., 2011. Screening risk assessment tools for assessing the environmental impact in an abandoned pyritic mine in Spain. Sci. Total Environ. 409, 692–703. doi:10.1016/j.scitotenv.2010.10.056

Muntener, O., 2010. Serpentine and serpentinization: A link between planet formation and life. Geology 38, 959–960. doi:10.1130/focus102010.1

Nriagu, J.O., 1996. A History of Global Metal Pollution. Science 272, 223–224. doi:10.1126/science.272.5259.223

Parsons, M.B., Bird, D.K., Einaudi, M.T., Alpers, C.N., 2001. Geochemical and mineralogical controls on trace element release from the Penn Mine base-metal slag dump, California. Appl. Geochem. 16, 1567–1593. Doi: 10.1016/S0883-2927(01)00032-4

565 Peijnenburg, W.J.G.M., 2020. Implementation of Bioavailability in Prospective and
566 Retrospective Risk Assessment of Chemicals in Soils and Sediments. In: The Handbook of
567 Environmental Chemistry. Springer, Berlin. doi: 10.1007/698_2020_516.

568 Piatak, N.M., Parsons, M.B., Seal, R.R., 2015. Characteristics and environmental aspects of
569 slag: A review. Appl. Geochem. 57, 236–266. doi:10.1016/j.apgeochem.2014.04.009

570 Piatak, N.M., Seal, R.R., Hammarstrom, J.M., 2004. Mineralogical and geochemical controls
571 on the release of trace elements from slag produced by base- and precious-metal smelting
572 at abandoned mine sites. Appl. Geochem. 19, 1039–1064.
573 doi:10.1016/j.apgeochem.2004.01.005

574 Pinsino, A., Matranga, V., Roccheri, M.C., 2012. Manganese: A New Emerging Contaminant
575 in the Environment. In: Environmental Contamination, Dr. Jatin Srivastava (Ed.), ISBN:
576 978-953-51-0120-8, InTech, pp. 17-36. Available from:
577 http://www.intechopen.com/books/environmental-contamination/manganese-a-new-
578 emerging-contaminant-in-the-environment. doi:10.5772/31438

579 Pinto, M., Rodriguez, M., Besga, G., Balcazar, N., Lopez, F.A., 1995. Effects of Linz-
580 Donawitz (LD) slag on soil properties and pasture production in the Basque country
581 (Northern Spain). N. Z. J. Agric. Res. 38, 143–155. doi:10.1080/00288233.1995.9513113

582 Pyatt, F.B., Pyatt, A.J., Walker, C., Sheen, T., Grattan, J.P., 2005. The heavy metal content of
583 skeletons from an ancient metalliferous polluted area in southern Jordan with particular
584 reference to bioaccumulation and human health. Ecotoxicol. Environ. Saf. 60, 295–300.
585 doi:10.1016/j.ecoenv.2004.05.002

586 R Core Team (2020). R: A language and environment for statistical computing. R Foundation
587 for Statistical Computing, Vienna, Austria. URL https://www.R-project.org/.

588 Riley, A.L., Mayes, W.M., 2015. Long-term evolution of highly alkaline steel slag drainage
589 waters. Environ. Monit. Assess. 187. doi:10.1007/s10661-015-4693-1

590 Roadcap, G.S., Sanford, R.A., Jin, Q., Pardinas, J.R., Bethke, C.M., 2006. Extremely Alkaline
591 (pH > 12) Ground Water Hosts Diverse Microbial Community. Ground Water 44, 511–
592 517. doi:10.1111/j.1745-6584.2006.00199.x

593 Seignez, N., Bulteel, D., Damidot, D., Gauthier, A., Potdevin, J.L., 2006. Weathering of
594 metallurgical slag heaps: multi-experimental approach of the chemical behaviours of lead
595 and zinc. WIT Press, 31–40. doi:10.2495/WM060041

596 Simkiss, K., Taylor, M.G., 1994. Calcium magnesium phosphate granules: atomistic
597 simulations explaining cell death. J. Exp. Biol. 190, 131–139.

598 Tossavainen, M., Engstrom, F., Yang, Q., Menad, N., Lidstrom Larsson, M., Bjorkman, B.,
599 2007. Characteristics of steel slag under different cooling conditions. Waste Manag. 27,
600 1335–1344. doi:10.1016/j.wasman.2006.08.002

601 Tylecote, R.F., 1987. The Early history of metallurgy in Europe. Addison-Wesley Longman,
602 Limited, pp. 391.

603 US EPA, 2007. Ecological Soil Screening Levels for Manganese. Interim Final. OSWER
604 Directive 9285.7-71. United Sates Environmental Protection Agency, Washington.

605 Walna, B., Spychalski, W., Ibragimow, A., 2010. Fractionation of iron and manganese in the
606 horizons of a nutrient-poor forest soil profile using the sequential extraction method. Pol. J.
607 Environ. Stud. 19.

608 Wilson, L.J., 1994. Literature review on slag leaching. Canada Centre for Mineral and Energy
609 Technology, Mineral Sciences Laboratories Division Report 94-3 (CR), Ottawa.

610

611 **Table captions**

612

613 **Table 1.** Metal concentrations ($\mu g.g^{-1}$) in soils from slag heaps and reference sites of the
614 Berthelange district and in slags (bulk) from the Antorpe 9 repository. [a]: data from
615 Crommentuijn et al. (2000). [b]: ecological soil screening level (Eco-SSL) from the US EPA
616 (2007).

617

618 **Table 2.** Chemical composition (mean ± standard deviation, SD) of slag-forming minerals
619 and glass obtained by EPMA (% in weight).

620

621 **Figure captions**

622

623 **Fig. 1.** A: map of the Berthelange ancient metallurgical district. Green areas are forests, red
624 dots correspond to archaeologically referenced slag deposits (from Forlin and Laurent, 2014)
625 and white stars correspond to the investigated slag heaps. B: photograph of the Antorpe 9 slag
626 heap. C: sampling map of the Antorpe 9 heap.

627

628 **Fig. 2.** Diffractograms. A: slag; B: bulk soil (SP8, 40-60 cm); C and D: clay fraction in soil
629 (SP8, 40-60 cm and SP4 80-100 cm, respectively); E: photograph of glass slide with clay
630 fraction without serpentine (SP10 0-20 cm); F and G: photograph of glass slide with clay
631 fraction containing serpentine (SP4, 80-100 cm and SP8 40-60 cm, respectively).

632

633 **Fig. 3.** Left (A to C): representative view of mineral-rich slag material from Antorpe 9. Right
634 (D to E): detailed view of a spherical metallic Fe particle trapped within slag from Antorpe 9.
635 A and D: BSE images; B and E: interpretative map of the mineral phases based on WDS and
636 compositional maps, respectively; C and F: Mn X-ray composition map based on WDS and
637 EDS, respectively. Brightness correlates with Mn content.

638

639 **Fig. 4.** Total (black bars) and extractable (white bars) manganese concentrations ($\mu g.g^{-1}$), the
640 organic matter content expressed in % (dashed line) and the pH value and observed slag
641 content (%) at each sampling point. The NW-SE transect is represented in the left panel (A),
642 and NE-SW is represented in the right panel (B). Different letters correspond to significant
643 differences (p-value<0.05). Code for slag abundance: AA (very abundant, *i.e.*, more than

644 50%), A (abundant, *i.e.*, between 25 and 50%), F (common, *i.e.*, between 20 and 25%), R
645 (rare, *i.e.*, between 10 and 20%), and T (trace, *i.e.*, less than 10%).

646

647 **Fig. 5.** A: Time course of snail growth (fresh weight) during the 4-week exposure to control
648 conditions (C) and to surface soils from site Antorpe 9. No significant difference (*p*-
649 value<0.05) between treatments was identified. B: Mn bioaccumulation in *C. aspersus* foot
650 (white) and viscera (black) (expressed in body burdens, $\mu g.snail^{-1}$) after exposure (for 28
651 days) to control conditions (C) and to surface soils from site Antorpe 9. t0 corresponds to the
652 metal body burdens in snails at the beginning of the experiment. For each snail part, different
653 letters correspond to significant differences (*p*-value<0.05).

654

655 **Table 1.**

656

	As	Ca	Cd	Co	Cu	Fe	Mg	Mn	Ni	Pb	Zn
Ref 1	13.3	268.6	<DL	8.3	11.7	16,811.6	1402.7	483.5	12.4	41.4	33.2
Ref 2	26.2	403.7	<DL	16.8	20.3	32,814.5	1390.4	789.2	21.3	48.9	62.9
Ref 3	19.2	335.4	<DL	16.4	15.4	25,574.8	1849.5	1146.5	18.5	28.2	47.6
Mercey-le-Grand 16	21.9	995.7	<DL	14.4	19.7	36,936.9	1663.0	1172.4	20.6	31.0	69.1
Ferrières 7	23.3	775.9	<DL	22.4	19.0	35,746.0	1850.6	1208.2	25.9	26.6	195.7
Dampierre 19	23.1	5461.2	0.6	15.0	21.3	27,745.6	1622.5	1422.5	24.4	29.8	61.2
Ferrières 8	35.4	797.4	0.3	22.5	21.0	40,902.3	1704.1	2088.4	32.3	31.6	135.7
Mercey-le-Grand 17	25.0	573.8	<DL	18.3	25.0	57,745.1	1391.5	2104.3	23.4	30.7	91.6
Petit-Mercey 25	57.5	3807.3	<DL	24.0	29.5	60,975.6	1600.6	2236.7	31.0	40.3	104.1
Louvatange 2	20.0	923.2	0.8	18.1	25.3	38,756.5	1294.2	2602.0	24.6	28.6	78.0
Dampierre 15	9.5	1075.6	<DL	14.3	16.9	32,110.0	1051.2	3165.8	16.9	31.2	70.2
Antorpe 22	30.1	3369.2	0.2	20.4	38.8	82,160.3	2027.5	3207.0	36.4	38.3	121.0
Dampierre 9	16.8	2152.3	<DL	16.4	26.3	52,950.5	1383.0	4709.2	20.3	55.2	87.2
Antorpe 9	51.8	6618.9	2.2	37.9	65.4	137,095.6	1553.7	8575.6	64.8	41.7	244.8
Maximum Permissible Concentration [a]	34.0		1.6	20.0	40.0			450 [b]	30.0	50.0	50.0
Antorpe 9 Slag #1	<DL	12,665.0	3.3	6.9	86.3	149,243.0	3296.6	17,590.5	27.3	11.5	27.2
Antorpe 9 Slag #2	<DL	14,899.2	3.3	10.8	87.4	154,248.9	3759.9	22,070.9	31.2	13.3	36.0
Antorpe 9 Slag #3	<DL	18,485.5	2.9	6.2	76.4	137,505.3	3436.2	11,135.5	25.0	9.0	28.8

657

658 **Table 2.**

659

	SiO2	*K2O*	*Na2O*	*P2O5*	*MnO*	*Al2O3*	*CaO*	*MgO*	*TiO2*	*FeO*	*Cr2O3*	*NiO*	*Total*
Glass (n=4)													
mean	40.16	3.12	0.25	1.55	1.69	20.23	9.07	0.02	1.22	22.35	0.01	0.02	99.68
SD	2.68	0.73	0.05	0.20	0.08	2.85	1.46	0.02	0.10	2.30	0.01	0.03	0.21
Fayalite (n=7)													
mean	29.24	0.07	0.01	0.52	4.51	0.59	0.51	1.00	0.13	63.72	0.02	0.01	100.32
SD	0.43	0.11	0.02	0.38	0.88	0.76	0.11	0.60	0.07	1.25	0.02	0.01	0.60
Leucite (n=3)													
mean	55.10	18.65	0.12	0.15	0.14	25.52	0.11	0.02	0.06	2.15	0.01	0.00	102.02
SD	1.85	1.10	0.03	0.18	0.14	0.37	0.12	0.01	0.03	2.31	0.01	0.00	0.50
Spinel (n=4)													
mean	3.01	0.13	0.02	0.02	1.56	49.23	0.08	0.25	2.41	44.60	1.02	0.00	102.32
SD	1.94	0.15	0.03	0.02	0.07	2.57	0.02	0.11	0.85	3.23	0.59	0.01	1.07
Wustite (n=2)													
mean	3.47	0.04	0.02	0.73	0.68	7.65	0.55	0.08	0.59	87.11	0.02	0.01	100.95
SD	2.19	0.01	0.02	0.58	0.06	7.93	0.39	0.02	0.18	5.13	0.01	0.01	1.83
Metallic Fe (n=2)													
mean	0.87	0.03	0.00	1.46	0.13	1.49	0.08	0.03	0.05	125.06	0.08	0.05	129.30
SD	0.39	0.03	0.00	1.91	0.15	2.10	0.10	0.02	0.06	1.89	0.12	0.07	1.54
Fe oxides (n=4)													
mean	2.21	0.01	0.04	0.09	0.05	0.01	0.02	0.02	0.01	87.65	0.01	0.02	90.12
SD	1.11	0.01	0.05	0.18	0.02	0.01	0.01	0.02	0.01	1.66	0.01	0.01	0.79
Fe hydroxides (n=4)													
mean	6.53	0.07	0.09	0.64	0.29	0.55	0.11	0.03	0.00	73.32	0.01	0.03	81.65
SD	4.08	0.04	0.10	0.77	0.23	1.06	0.04	0.03	0.01	2.86	0.01	0.03	1.45

660

Figure 1.

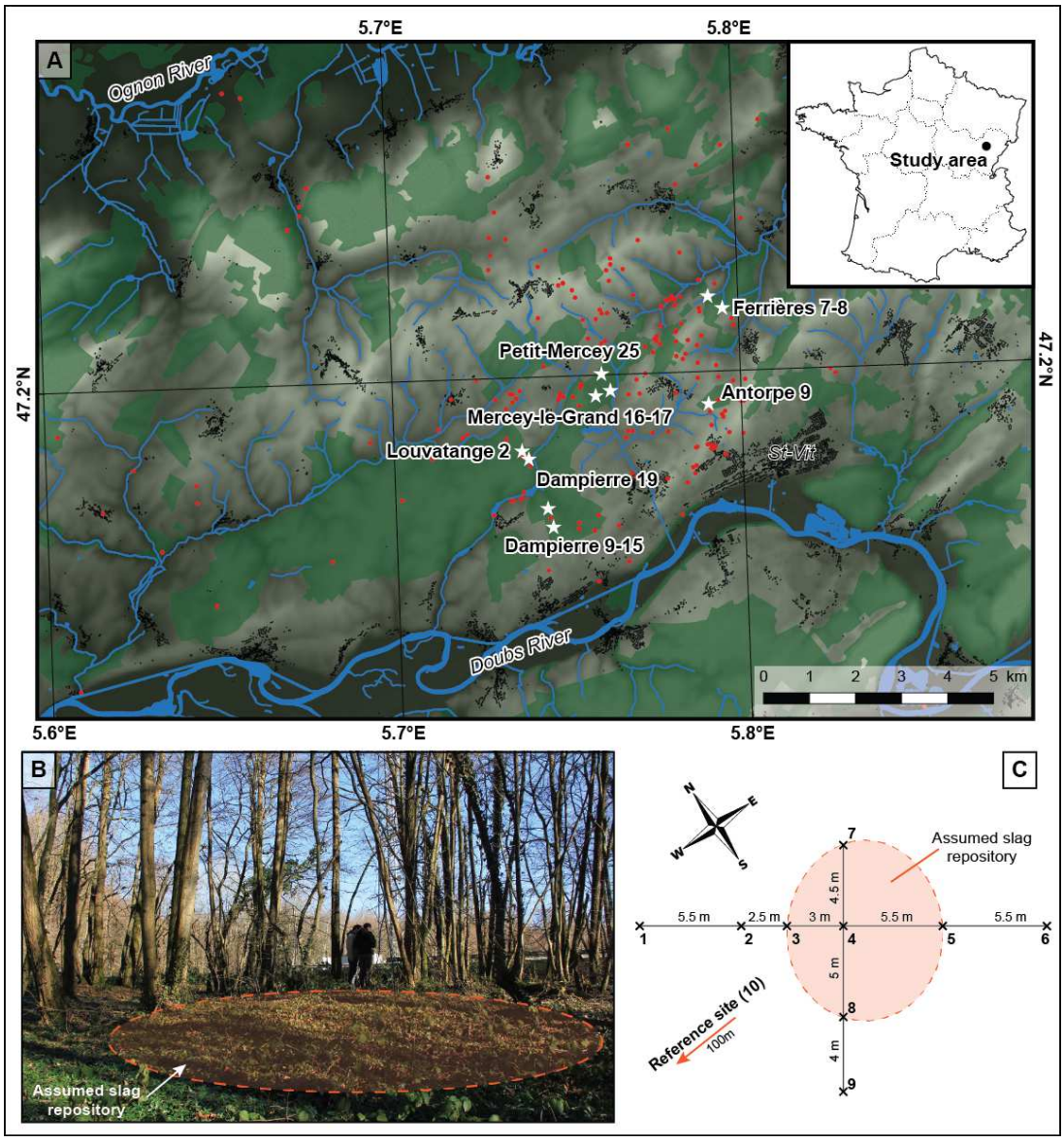

663

664

665

Figure 2.

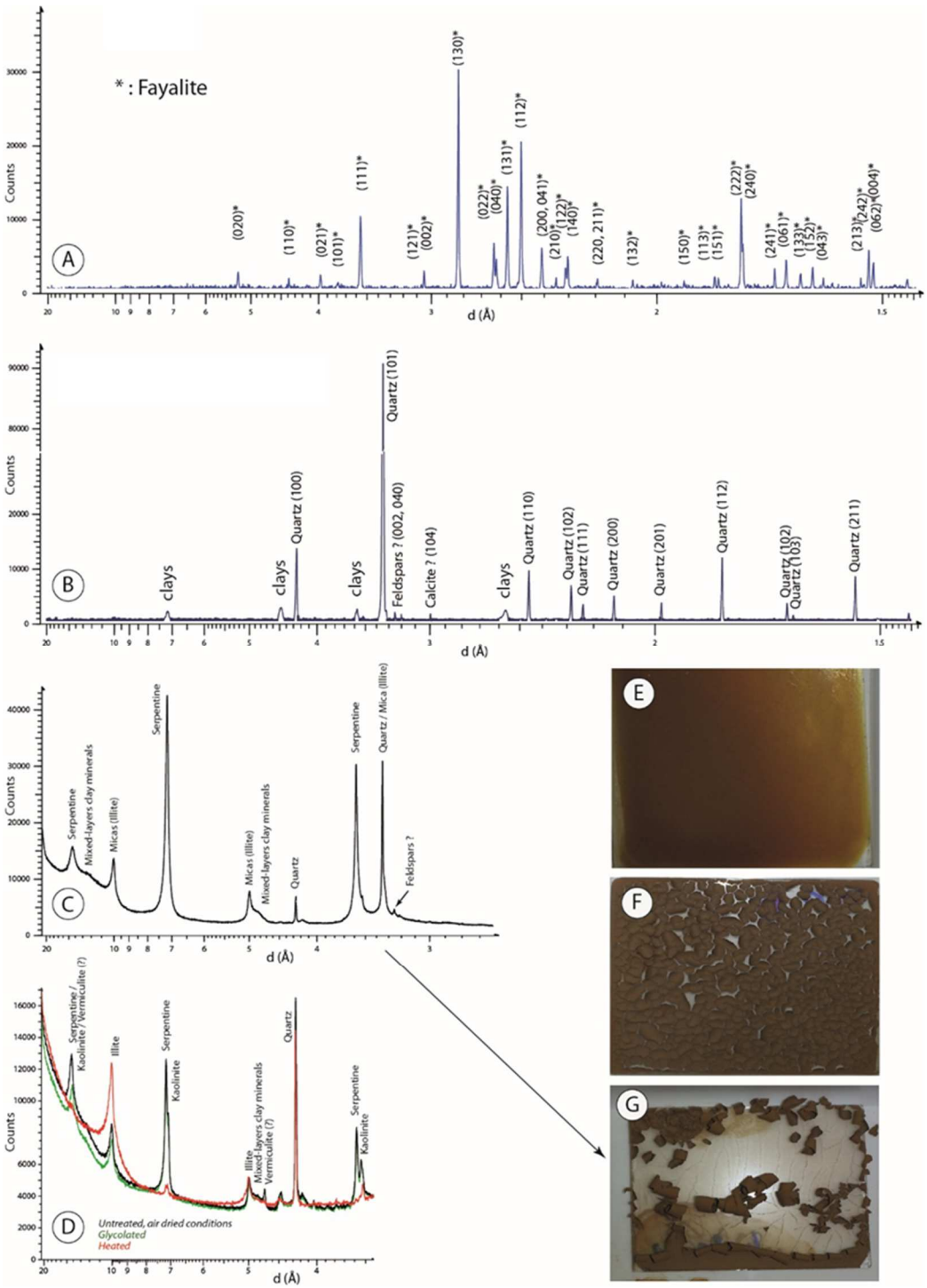
A
*: Fayalite
Counts
d (Å)
(020)*
(110)*
(021)*
(101)*
(111)*
(121)*
(002)*
(130)*
(022)*
(040)*
(131)*
(112)*
(200, 041)*
(210)*
(122)*
(140)*
(220, 211)*
(132)*
(150)*
(113)*
(151)*
(222)*
(240)*
(241)*
(061)*
(133)*
(152)*
(043)*
(213)*
(242)*
(062)*
(004)*
B
clays
Quartz (100)
Quartz (101)
Feldspars ? (002, 040)
Calcite ? (104)
Quartz (110)
Quartz (102)
Quartz (111)
Quartz (200)
Quartz (201)
Quartz (112)
Quartz (102)
Quartz (103)
Quartz (211)
C
Serpentine
Mixed-layers clay minerals
Micas (illite)
Quartz
Quartz / Mica (illite)
Feldspars ?
D
Serpentine / Kaolinite / Vermiculite (?)
Illite
Kaolinite
Untreated, air dried conditions
Glycolated
Heated
E
F
G

Figure 3.

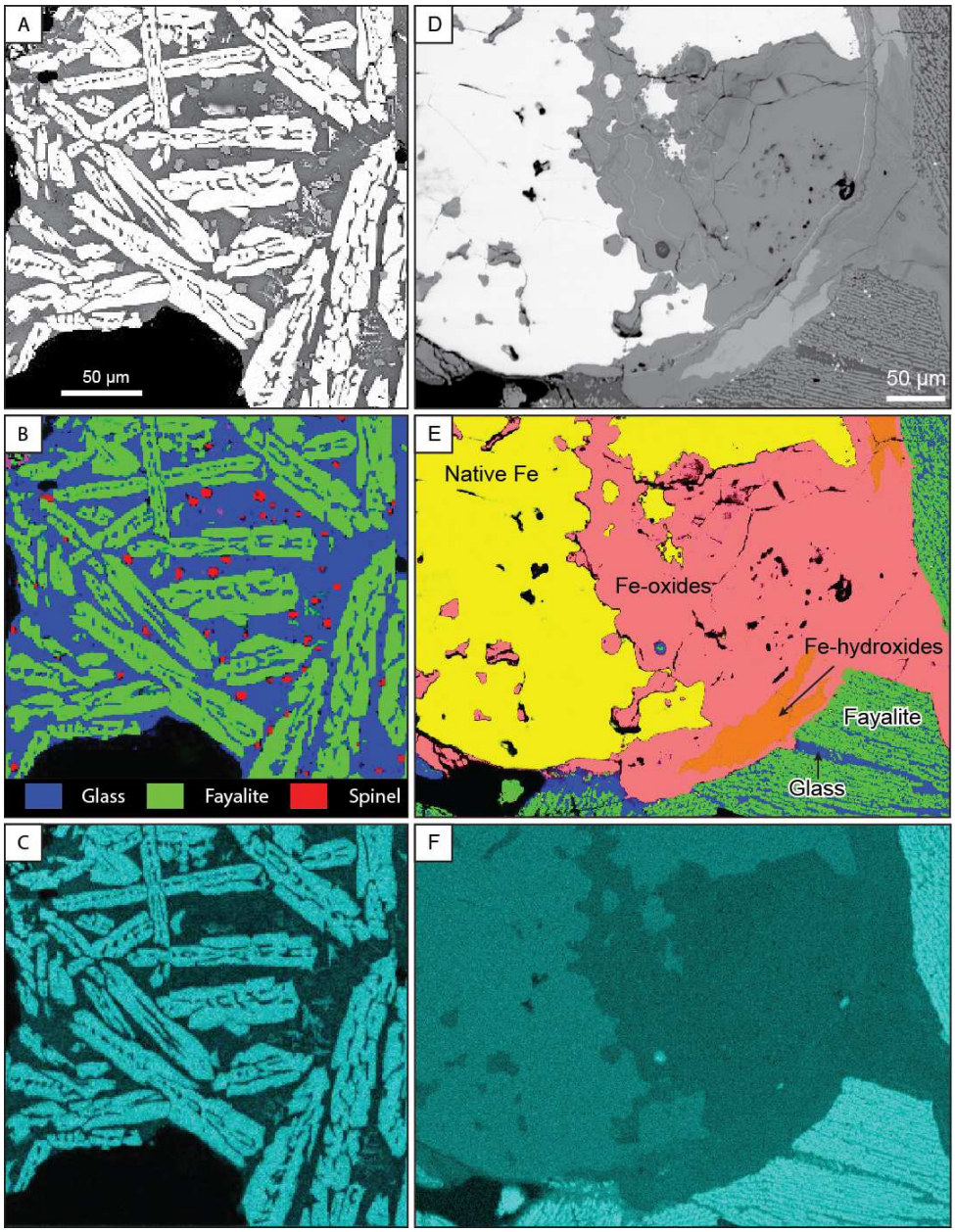
A
50 µm
D
50 µm
B
Glass
Fayalite
Spinel
E
Native Fe
Fe-oxides
Fe-hydroxides
Fayalite
Glass
C
F

674 **Figure 4.**

675

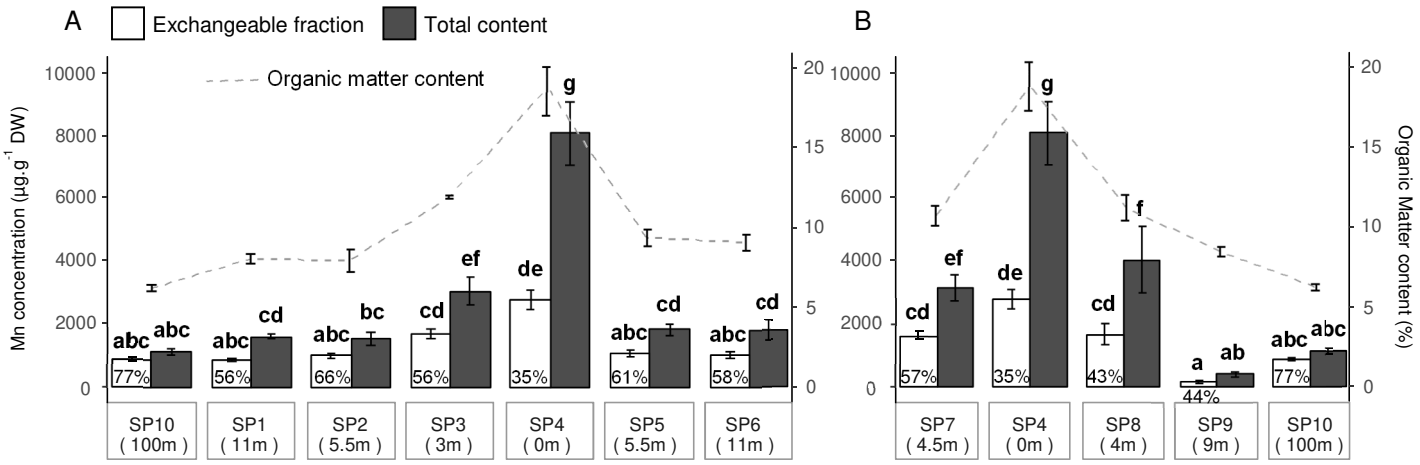

pH	4.76±0.09 **a**	4.87±0.09 **ab**	5.02±0.11 **abc**	5.11±0.01 **bcd**	5.34±0.08 **de**	5.07±0.16 **bcd**	5.42±0.16 **e**	5.34±0.03 **de**	5.34±0.08 **de**	5.31±0.11 **cde**	5.09±0.06 **bcd**	4.76±0.09 **a**
Slags (%)	NA	T	T	AA	AA	T	T	F	AA	AA	T	NA

676

677

678

679 **Figure 5.**

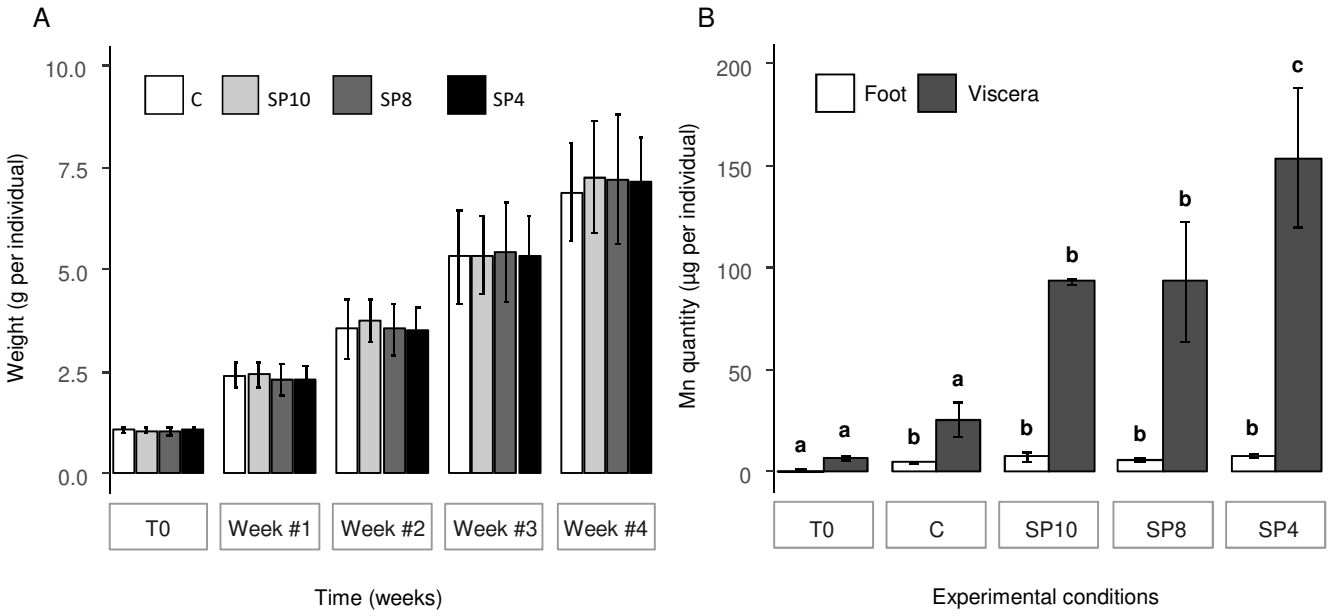

680

681

Graphical Abstract